

Influences of Process Parameter and Microstructural Studies in Friction Stir Welding of Different Alloys: A Review

Husain Mehdi*, R.S. Mishra
(Delhi Technological University, Delhi-110042, India)
*Email: husainmehdi4u@gmail.com

Abstract : Friction stir welding (FSW) is a relatively new solid state joining process that uses a non-consumable tool to join two different material without melting the workpiece material. Heat is generated by friction between the rotating tool and the workpiece material. This joining process is energy efficient, environment friendly and versatile. Friction stir welding (FSW) was developed for microstructural modification of metallic material. This review article provides an overview of effect of FSW/FSP mechanism responsible for the formation of weld, microstructure refinement, wear of FSW tool and mechanical properties. This review conclude with recommendations for future research direction.

Keywords: Process Parameter, Microstructural Studies, Friction Stir Welding, Different Alloys

INTRODUCTION

Friction stir processing (FSP)/FSW is a method of changing the properties of a metal through intense localized plastic deformation. This deformation is produced by forcibly inserting a non-consumable tool into the workpiece and revolving the tool in a stirring motion as it is pushed laterally through the workpiece. The antecedent of this technique, friction stir welding is used to join multiple piece of metal without creating the heat affected zone typical of fusion welding. In friction stir welding the tool usually has a large

diameter shoulder and a small threaded pin. The plate to be welded are aligned together and clamped using fixture. A Cylindrical hole is drilled at one end of the workpiece on the centerline and the pin is inserted into the hole, with the shoulder in contact with the top surface of the workpiece. The tool is rotating at high speed as it is moved along the weld centerline. Heat is generated by friction between the tool and the workpiece and by the plastic deformation of the workpiece material. A schematic diagram of the friction stir welding system is shown in figure 1.

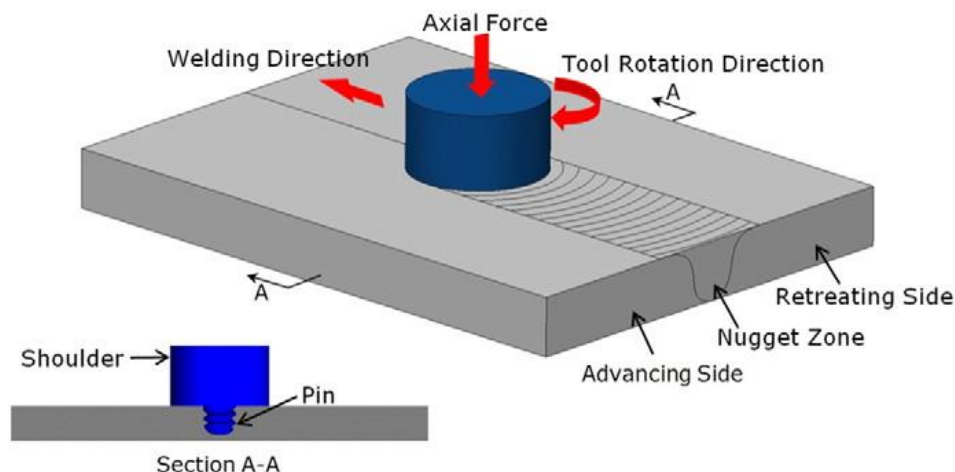


Figure 1:- Friction Stir Welding

LITERATURE REVIEW

The review is presented in a tabular form. 40 research paper related to friction stir welding and friction stir processing of aluminum alloy and other alloys have been

considered. The review table given below explain the detail of materials and processing parameters considered by earlier authors.

S.No	Author & year	Material Used	Processing Parameter	Conclusion												
1	Y.Wang et al [2007]	Al-4.0Y-4.0Ni-0.9Co Alloy	<table border="1" style="width: 100%; border-collapse: collapse;"> <thead> <tr> <th style="text-align: center;">Weld</th> <th style="text-align: center;">Tool Rotation (r.p.m)</th> <th style="text-align: center;">Speed (mm /s)</th> <th style="text-align: center;">Tilt angle</th> </tr> </thead> <tbody> <tr> <td style="text-align: center;">Weld-1</td> <td style="text-align: center;">1000</td> <td style="text-align: center;">51</td> <td style="text-align: center;">0⁰</td> </tr> <tr> <td style="text-align: center;">Weld-2</td> <td style="text-align: center;">1200</td> <td style="text-align: center;">51</td> <td style="text-align: center;">0⁰</td> </tr> </tbody> </table>	Weld	Tool Rotation (r.p.m)	Speed (mm /s)	Tilt angle	Weld-1	1000	51	0 ⁰	Weld-2	1200	51	0 ⁰	Significant improvement in ductility was observed after FSW of UFG Al-4.0Y-4.0Ni-0.9Co alloy with a slight decrease in strength. FSW leads to homogenization of the microstructure and change in the shape of intermetallic particles.
Weld	Tool Rotation (r.p.m)	Speed (mm /s)	Tilt angle													
Weld-1	1000	51	0 ⁰													
Weld-2	1200	51	0 ⁰													
2	Indrajit Charit et al [2002]	7475 Al alloy sheets	Two sheets, 2.5 mm thick, were lap joined using two welding conditions, i.e., (a) single-pass and (b) sixpass joints. The FSW parameters were kept the same for both weld procedures. Overlap between passes was one-half of the pin tool diameter. A series of short (5 and 30 min) annealing experiments were performed to evaluate the effect of thermal exposure on the weld joint microstructure.	The microstructure in the weld HAZ is stable and retains superplastic properties. The high strength weld nugget, because of the higher flow stress at 783 K compared to the parent metal (16–18 MPa versus 2–9 MPa), is unlikely to deform during super plastic forming (SPF).												
3	V. Jeganathan Arulmoni et al [2015]	99.99% Cu with carbon nano tube	The tool Material used is H13 steel with shoulder diameter 15mm, threaded pin diameter 8 mm, pin length 2.5 mm with tool rotational speed 960 rpm, tool angle 2 and table traverse speed 25 m / min.	It investigate the parameters affecting the friction stir welding of copper with carbon nano tube and enhancement of the microstructure, hardness and tensile properties of the composite material with single pass, double passes and triple passes.												
4	Jiye Wang et al [2014]	Titanium alloy Ti-6Al-4V	Processing parameters of 1000 rpm and 25 mm per minute were applied during FSW.	Fracture failure was observed in the CY16 tool. Micro cracking was observed in the WC411 tool with improved fracture toughness, and the crack propagation in the tool was inhibited. Tool degradation due to plastic deformation was observed in the W-La tool, and can be reduced by increasing the pin diameter												
5	J-Q-Su et al [2002]	Aluminum alloy 7050-T65	The pin rotation speed was 350 rpm and the pin travel speed was 15 mm/min	Compared to parent material microstructure, the strengthening precipitates have coarsened severely and the precipitate free zone along the grain boundaries has increased by factor of five during friction stir welding, The original base metal grains structure is completely eliminated and replaced by a very fine equiaxed grain structure in the dynamic re-crystallized zone (DXZ).												
6	V. Jeganathan et al [2014]	Aluminum Alloy	The rotational speeds (800, 1250, 1600 and 2000rpm) and two traverse speeds 31.5 and 63 mm/min were tried.	It was observed that when the target depth is too large, the shoulder of tool pushes way all the preplaced SiC particles, and basically no surface composite is formed. Too small depth was also ineffective to mix SiC particles into aluminum alloy.												
7	S.Jana, et al [2009]	Al-7Si-0.6 Mg alloy	The FSP tool had a pin height of 1.9 mm, a diameter of 4 mm at mid-pin height and a tool	FSP improved the fatigue life of a cast Al-7Si-0.6 Mg alloy by a												

			shoulder diameter of 12 mm. Therefore, the FSPed region had a thickness of 2.0 mm. A process parameter combination of 2236 rpm and 2.33 mm/s was used for the FSP runs	factor of 15 when specimens were tested at the same stress level and at a stress ratio of R = 0.
8	Z.Y.Ma et al [2006]	cast A356 aluminum	Tool rotation rate of 300,500,700 and 900 rpm and a traverse speed of 51, 102 and 203 mm/min is used.	Higher tool rotation rate creates a more homogeneous microstructure. The varied distribution pattern, size, and volume fraction of Si particles at different locations within the FSP zone indicates inhomogeneous material flow
9	Patrick B. Berbon [2001]	Aluminum alloys (Al-10%Ti-2%Cu and Al-10%Ti-2%Ni)	Friction stir processing was performed at the Rockwell Science Center using conventional friction stir weld tools and weld parameters.	The homogeneity increased dramatically via friction stir processing. There are no traces of the pure aluminum area left and the largest intermetallic particles have a small size. The strength is very high at the lower temperature. The ductility however is very poor.
10	Z.Y.Ma et al [2002]	7075Aluminum alloy	Two different processing parameters, i.e., 4 ipm/400 rpm and 6 ipm/350 rpm were used to generate the microstructures with different grain sizes.	Grain size will decrease in the temperature range of 420-530 and strain rate range of 1×10^{-3} to 10^{-1} . For the $3.8 \mu\text{m}$ 7075Al alloy, super plastic elongation of 1250% were obtained at 480 in the strain rate range of 3×10^{-3} to 3×10^{-2} s ⁻¹ , whereas the $7.5 \mu\text{m}$ 7075Al alloy exhibited a maximum ductility of 1042% at 5000 and 3×10^{-3} s ⁻¹
11	Z.Y.Ma et al [2003]	Al-4Mg-1Zr Alloy	A ram speed of 3 mm/s and temperatures of 400 - 550 C was used.	Fine microstructure with a grain size of 1.5 μm and uniform distribution of fine Al ₃ Zr dispersoids was obtained in Al-4Mg-1Zr alloy via FSP.
12	R.S Mishra et al [2003]	Al-SiC Composite	Tool transfer rate of 25.4 mm/min and 101.6 mm/min is used for different target depth i.e. 1.78mm, 2.03mm, 2.28mm	When the target depth is too large (2.28mm), the shoulder of tool pushed away all the preplaced SiC particles and basically no surface composite formed. Too small target depth (1.78mm) was also ineffective to mix SiC particles into Al-alloy. A target depth of 2.03 mm resulted in incorporation of SiC particles in Aluminum matrix.
13	S. Jana et al [2007]	Cast Al-Alloy of F357	The tool rotation rate was 2236 rpm, and tool traverse speeds were 0.42, 0.98, 2.33 and 3.67 mm/s.	The multiple pass does not resulted in Si particles refined beyond a certain limit. The multi pass run of second configuration indicate that the extent of AGG can be reduced if the material is FSPed multiple times
14	S. Jana et al [2010]	Al-7Si-0.6Mg alloy	Tool rotation rate of 2236 rpm and travel speed of 2.33 mm/s	FSP led to a five times improvement in fatigue life for a hypoeutectic Al-Si-Mg cast alloy. The cast fatigue specimen showed a life of 45500 cycles. As expected crack were noted to have originated at porosity when the test was stopped after the first 5000 cycles which implies a 10% or lower crack initiation periods.
15	Z.Y.Ma et al [2005]	Al-4Mg-1Zr	The traverse speed of the tool 4ipm and the rotation rate of the tool 350 rpm was used	A maximum super plastic ductility of 1280 pct was observed at 525C and initial strain rate of 1×10^{-1} s ⁻¹ . The strain rate sensitivity of

				both as- extruded and FSP Al-4Mg-1Zr increased continuously with increasing strain rate from 1×10^{-3} s ⁻¹ to 1 s ⁻¹ .
17	S.R Sharma [2004]	A356 Alloy	One plate was processed using a standard FSW pin at 900 rpm and a traverse speed of 203.2 mm per minute and the other plate was processed using a tri-flute pin at 700 rpm and 203.2 mm per minute.	Fatigue life improvement was attributed to significant refinement, homogenization of the microstructure and the elimination of porosity. FSP resulted in a significant breakup and uniform distribution of Si particles in the aluminum matrix as well as elimination of porosity.
18	Jian-Qing Su et al [2011]	Copper	The tool was tilted $\sim 2.5^\circ$ opposite the traveling direction during a single processing pass on the Cu sheet at 800 rpm and a travel speed of 120 mm/min.	The material flow in a very thin layer around pin tool resulted in severe strain heterogeneity giving rise to highly concentrated micro plastic deformation at location with in this layer. Under such circumference a very high density of micro band structure were formed.
19	Nilseh Kumar et al [2012]	Al-Mg-Sc alloy	The alloy was processed in as-received and aged (563 K, 22 hours) conditions and at three different tool rotation rates: 800, 400, and 325 rpm.	The grain size varied from 0.89 to 0.39 μm depending on the processing and initial thermos-mechanical condition of the alloy. The grain size reduction was observed with increase in Zener-Holloman parameter.
20	Z.Y.Ma et al [2006]	Al-Si alloy A356	Five-pass FSP with a tool rotation rate of 700 rpm and a traverse speed of 203 mm/min was performed using a tri-flute pin.	Overlapping FSP did not affect the size, aspect ratio and distribution of the Si particles. The Si particles broken by FSP were uniform distributed in the entire processed zones created by multi pass FSP.
21	Z.Y.Ma et al [2004]	Al-Si alloy A356	Single pass FSP with a tool rotation rate of 700 rpm and transverse speed of 203 mm/min was performed on 6.35 mm	The flow stress of FSP A356 was significantly lower than that of cast A356 FSP. Maximum super plasticity of 650% was obtained at 530C and an initial strain rate of 1×10^{-3} s ⁻¹ in FSP A356.
22	Z.Y.Ma et al [2009]	7075 Al Alloy	A Tool rotation rate of 600 rpm and a traverse speed of 102 mm/min was used.	A shift to higher optimum temperature was observed in the two pass FSP 7075Al. Maximum superplastic elongation of 1220% was achieved at 480C and an initial strain rate of 10 ⁻² s ⁻¹ in the center region of second pass in the two pass FSP 7075Al
23	Z.Y.Ma et al [2003]	Al-Si alloy A356	Tool rotation rate of 300,700, 900 and 1100 rpm and a traverse speed 2 and 8 ipm	The strength of FSP A356 increased with increasing tool rotation rates. For the standard pin, a maximum strength was observed at a tool rotation rates of 900 rpm
24	Jianqing Su et al [2013]	Ti-6Al-4V alloy	Tool rotational speed (800-1000 rpm) and tool traverse speed (1-4 IPM) was used in this work.	The higher yield and ultimate tensile strength of 1067 MPa and 1156MPa without any losses of ductility were achieved in 900 rpm/4IPM sample having the smallest prior β grains size of $\sim 12\mu\text{m}$
25	Z.Y. Ma et al [2010]	Al-4Mg-1Zr alloy with grain size of 0.7 μm	Tool rotation rate was 600 rpm and tool transverse speed 25.4 mm/min used.	High strain rate and low temperature super plasticity of greater than 1200% work observed at 10 ⁻² to 1×10^{-1} s ⁻¹ and 300-

				350C even at 425C a super plasticity of 1400% was achieved at an exception alloy high strain rate of 1s-1.
26	Omar.S.Salih et al [2015]	Aluminium matrix composites (AMCs)	Tool rotation speed was 600, 800 and 1000 rpm and tool transverse speed was 40, 80 mm/min used	Welding parameters such as tool rotation, speed, transverse speed and axial force have a significant effect on the amount of heat generation and strength of FSW joints. Microstructural evaluation showed the formation of tunnel defect due to inappropriate flow of plasticized metal
27	S.R Ren et al [2007]	6061Al-T651	Tool rotaion speed was 400,600, 800, 1200 and 1600 rpm whereas tool transverse speed was 100 and 400 mm/min were used.	Under the welding parameters investigated in this study, the traverse speed appears to be a dominant factor in determining the tensile properties and fracture mode of the welds .FSW 6061Al-T651 joints welded at 400 mm/min exhibited higher strength with a 45 shear fracture, whereas a lower tensile strength with nearly vertical fractures were observed for the samples welded at 100 mm/min.
28	N.Kamp et al [2006]	AA7449 aluminium alloy.	The interfacial energy of the different phases and the diffusion rates was taken	A numerical analytical model based on the Kampmann and Wagner numerical (KWN) model has been developed to predict the precipitate dis-tribution evolution in 7xxx alloys during complex processing.
29	R.Nandan et al [2007]	Mild Steel	Pin radius, pin length, weld speed, and rotational speed are 3.95 mm, 6.22 mm, 0.42 mm/sec and 450 rpm respectively.	Three-dimensional temperature and plastic flow fields during FSW of mild steel have been calculated by solving the equations of conservation of mass, momentum and energy. The spatially variable non-Newtonian viscosity was determined from the computed values of strain rate,
30	M. Maalekian et al [2008]	Steel Bar having Composition 0.75C,1.02Mn, 0.28Si, 0.11Cr, 0.05Ni, 0.015S, 0.009P, 0.08Cu	function of process parameters $q = 2\pi.n.e.\mu.P$ Where q= heat flux, μ =Coulomb coefficient of friction, n= rotational speed, e = Amplitude, P= pressure	The heat-generation rate in orbital friction welding of steel bars is analyzed using four different methods; constant Coulomb friction, sliding-sticking friction, the experimentally measured power data and an inverse heat conduction approach.
31	L.Commin et al [2009]	AZ31 Magnesium Alloy	Four welding condition (1000 rpm/200 mm min, 1300 rpm/300 mm min 1400 rpm/700 mm min, and 600 rpm/2000 mm min was used.	Stress levels observed are higher on the retreating side. Grain growth is observed with an increase in the processing parameters that promote heat generation. FSW induced lower tensile mechanical properties for this hot-rolled base metal alloy.
32	S.Mironov et al [2009]	Pure Titanium	low tool rotational speed of 200 rpm	The microstructure evolution during friction stir welding of commercial purity titanium was studied. Material flow was found to be close to the simple-shear deformation and arose mainly from the prism slip. The grain structure evolution was shown to be a complex process including several stages.

33	L. Fratini et al [2010]	AA7075-T6	The tool rotation rate were 715 and 1500 rpm, and tool traverse speeds were 105 and 214 mm/min	The effects of in process cooling on the material characteristics and joint performance have been presented on AA7075-T6
34	S. Mironov et al [2011]	S31254 superaustenitic stainless steel	A tool rotational speed of 400 r.p.m. and a tool travel speed of 30 mm/min	The structural response of a typical low stacking fault energies (SFE) material S31254 to FSW has been studied. Formation of the final stir zone (SZ) microstructure was deduced to be primarily governed by discontinuous recrystallization occurring during the FSW cooling cycle.
35	Y.S. Sato et al [2004]	Al Alloy 1100	Rotation speed of the welding tool was 500 rpm, and the traveling speed was 12 mm/sec	Friction stir welding (FSW) was applied to an accumulative roll-bonded (ARBed) Al alloy 1100. FSW resulted in reproduction of fine grains in the stir zone and small growth of the ultrafine grains of the ARBed material just outside the stir zone.
36	G.R. Argade at al [2012]	Magnesium Alloy Mg-Y-Re	Tool rotation rate of 800 rpm and tool traverse speed of 25.4 mm/min.	Effect of grain refinement and heat treatment on corrosion behavior of a friction stir processed Mg-Y-RE alloy was studied. Different trends between microstructural conditions and corrosion behavior were observed with electrochemical testing and constant immersion testing.
37	G. Buffa et al [2011]	A 3D FE model, with general validity for different joint configurations, was used to simulate	Tool rotating speed and tilt angle were kept constant and equal to 500 rpm and 21, respectively. Three levels of advancing velocity, i.e. 100, 225 and 325 mm/min were selected.	A new numerical procedure for the prediction of the residual stress distributions in Friction Stir Welding processes is Studied.
38	Seung Hwan C. Park [2003]	304 stainless steel	Tool rotation rate 1400 rpm, tool traverse rate was at 1.3 mm/s and tool was tilted at 3.5 from vertical.	The microstructural observation revealed that sigma phase including the numerous stacking faults was formed at the advancing side of the stir zone.
39	C. Hamilton et al [2008]	AA6061-T6 Aluminum alloy	Range of tool rotation rate 50 to 550 rpm was used.	A thermal model of friction stir welding was developed that utilizes a new slip factor based on the energy per unit length of weld. The thermal model successfully predicts the maximum welding temperature over a wide range of energy levels
40	C. Hamilton et al [2009]	Al-Zn-Mg-Cu alloy	Tool rotation rate 225, 250, 300 and 400 rpm and constant weld velocity of 2.1 mm/sec was used.	In this work, the model successfully predicts the maximum welding temperatures and temperature distributions over the energy range investigated.

CONCLUSIONS

The mechanical properties of welded joint by friction stir welding are largely dependent on the combined effect of both the composition of alloying element and processing parameter, there for, the mechanical performance of friction stir welding joint should be evaluated accordingly. Past researcher showed that FSW is a potential welding process to achieve defect free joint. Welding parameter such as tool

rotation, transverse speed and axial force have a significant effect on the amount of heat generated and strength of FSW joints. Microstructure evaluation of FSW joints clearly shows the formation of new fine grains and refinement of reinforcement particles in the weld zone with different amount of heat input by controlling the welding parameter.

REFERENCES

- [1] Y.Wang, X.L Shi, R.S mishra, T.J Watson, "Friction stir welding of devitrified AL-4.0Y-4.0Ni-0.9Co alloy produced by amorphose powder", *Scripta Materialia* 56 (2007) 971-974.
- [2] Indrajeet Charit, Rajiv S. Mishra, Murray W. Mahoney, "Multi sheet structure in 7475 aluminum by FSW in concert with post weld superplastic forming", *Scripta Materialia* 47 (2002) 631-636.
- [3] V.Jeganthan Arulmoni, Ranganath M.S, R.S Mishra, "Effect of single and multi passes FSP on microstructure, hardness and tensile properties of a 99.99% Cu with carbon nano tube", *International Journal of advance research and innovation*, 3(1), 2015, 189-196.
- [4] Jiye wang, Jianqing Su, R.S Mishra, Ray Xu, John A. Baumann, "Tool wear mechanism in friction stir welding of Ti-6Al-4V", *wear* 321 (2014), 25-32.
- [5] J.Q. Su, T.W Nelson, R.S Mishra, M.Mahoney, "Microstructure investigation of friction stir welding 7050-T651 aluminum, *acta materialia*, 2002.
- [6] V.Jeganatham Arumoni, R.S Mishra, "Friction stir processing of Al-alloy for defence application, *International journal of advance research and innovation*, 2(2), 2014, 337-341.
- [7] S.Jana, R.S.Mishra, J.B Baumann, G. Grant, "Effect of stress ratio the fatigue behaviour of a friction stir processed cast Al-Si-Mg alloy, *Scripta Materialia* 61 (2009), 992-995.
- [8] Z.Y.Ma, S.R Mishra, R.S Mishra, "Effect of Friction Stir Processing on the microstructure of CastA356 Al", *Material Science and Engineering A* 433 (2006), 269-278.
- [9] Patric B. Berdon, Willam H. Bingel, R.S Mishra, "Friction Stir Processing: A Tool to homogenize nano composite Al Alloy, *Scripta mater*, 44 (2001), 61-66.
- [10] Z.Y.Ma, R.S Mishra, M.W. Mahoney," Super plastic deformation behavior of friction stir processed 7075Al alloy", *Acta Materialia* 50 (2002), 4419-4430.
- [11] Z.y. Ma, R.S.Mishra, M.W.Mahoney, R.Grimes," High strain rate super plasticity in friction stir processed Al-4Mg-1Zr alloy", *Material Science and Engineering A* 351 (2003) 148-153.
- [12] R.S Mishra, Z.Y.Ma, I. Charit, "Friction stir processing: A Novel technique for fabrication of surface composite", *Matrial Science and Engineering A* 341 (2003) 307-310.
- [13] S. Jana, R.S. Mishra, J.A Baumann, G. Grant, " Effect of process parameters on abnormal grain growth during FSP of a cast Al-Alloy", *Material Science and Engineering A*, 528 (2010) 189-199.
- [14] S.Jana, R.S Mishra, J.B Baumann, " Effect of friction stir processing on fatigue behavior of an investigation cast Al-7Si-0.6Mg alloy, *Acta Materialia*, 58 (2010) 989-1003.
- [15] Z.Y Ma, R.S.Mishra, M.W Mahoney, R. Grimes, "Effect of Friction Stir Processing on the the kinetic of superplastic deformation in an Al-Mg-Zr Alloy", *Metallurgical and Material Transaction*, 36A (2005), 1447-1458.
- [16] Z.Y Ma, R.S Mishra, "Cavitation in super plastic 7075 Al alloy prepared via friction stir processing, *Acta Materialia* 51 (2003) 3551-3569.
- [17] S.R Sharma, R.S Mishra, Z.Y Ma, "Effect of friction stir processing on fatigue behaviour of A356 Alloy", *Scripta Materialia* 51 (2004) 237-241.
- [18] Jian Qing Su, T.W Nelson, T.R. McNelley, "Development of Nano crystalline structure in Cu during Friction Stir Processing", *Material Science and Engineering A*, 525 (2011) 5458-5464.
- [19] Nilesh Kumar, R.S Mishra, " Ultrafined Grained Al-Mg-Sc Alloy via friction Stir Processing", *Metallurgical and Materials Transaction*, 44A (2013) 934-945.
- [20] Z.Y Ma, S.R Sharma, R.S Mishra, " Effect of Multipass Friction Stir Processing on Microstructure and tensile propeties of a Cast Al-Si Alloy", *Scripta Materialia*, 54 (2006) 1623-1626.
- [21] Z.Y. Ma, R.S Mishra, M.W Mahoney, " Superplasticity in Cast A356 induced via friction Stir Processing", *Scripta Materialia* 50 (2004) 931-935.
- [22] Z.y.Ma, R.S Mishra, F.C Liu, "Super plastic behaviour of Micro-region in two pass friction stir processing 7075Al alloy", *Materialia Science and Engineering A* 505 (2009) 70-78.
- [23] Z.Y.Ma, S.R Sharma, R.S Mishra, M.W Mahoney, " Micro structural modification of cast aluminum alloy via friction stir processing", *Material Science Forum*, vol 426-432 (2003) 2891-2896.
- [24] Jianqing Su, Jiye Wang, R.S Mishra, Ray Xu, " Microstructure and Mechanical Properties of Friction Stir Processing Ti-6Al-4V Alloy", *Material Science and Engineering A* 573 (2013) 67-74
- [25] Z.Y.Ma, F.C.Liu, R.S Mishra, " Superplastic deformation mechanism of ultrafined grained aluminum alloy produced friction stir welding", *Acta Materialia*, 58 (2010) 4693-4704.
- [26] Omar S. Salih, Hangan Ou, W.Sun, D.G McCartney, "A review of friction stir welding of aluminum matrix composite", *Material and Design* 86 (2015) 61-71.
- [27] S.R. Ren, Z.Y. Ma, L.Q. Chen, Effect of welding parameters on tensile properties and fracture behavior of friction stir welded Al-Mg-Si alloy, *Scripta Materialia*, 56(2007), 69-72.
- [28] N. Kamp, A. Sullivan, R. Tomasi, J.D. Robson, Modelling of heterogeneous precipitate distribution evolution during friction stir welding process, *Acta Materialia* 54 (2006) 2003-2014.
- [29] R. Nandan, G.G. Roy, T.J. Lienert, T. Debroy, Three-dimensional heat and material flow during friction stir welding of mild steel, *Acta Materialia* 55 (2007) 883-895.
- [30] M. Maalekian, E. Kozeschnik, H.P. Brantner, H. Cerjak, Comparative analysis of heat generation in friction welding of steel bars, *Acta Materialia* 56 (2008) 2843-2855.
- [31] L. Commin, M. Dumont, J.-E. Masse, L. Barrallier, Friction stir welding of AZ31 magnesium alloy rolled sheets: Influence of processing parameters, *Acta Materialia* 57 (2009) 326-334.
- [32] S. Mironov, Y.S. Sato, H. Kokawa, Development of grain structure during friction stir welding of pure titanium, *Acta Materialia* 57 (2009) 4519-4528.
- [33] L. Fratini, G. Buffa, R. Shivpuri, Mechanical and metallurgical effects of in process cooling during friction stir welding of AA7075-T6 butt joints, *Acta Materialia* 58 (2010) 2056-2067.
- [34] S. Mironov, Y.S. Sato, H. Kokawa, H. Inoue, S. Tsuge, Structural response of superaustenitic stainless steel to friction stir welding, *Acta Materialia* 59 (2011) 5472-5481.
- [35] Y.S. Sato, Y. Kurihara, S.H.C. Park, H. Kokawa, N. Tsuji, Friction stir welding of ultrafine grained Al alloy 1100 produced by accumulative roll-bonding, *Scripta Materialia* 50 (2004) 57-60.
- [36] G.R. Argade, K. Kandasamy, S.K. Panigrahi, R.S. Mishra, Corrosion behavior of a friction stir processed rare-earth added magnesium alloy, *Corrosion Science* 58 (2012) 321-326.

- [37] G. Buffa, A. Ducato, L. Fratini, Numerical procedure for residual stresses prediction in friction stir welding, *Finite Elements in Analysis and Design* 47 (2011) 470–476.
- [38] Seung Hwan C. Park, Yutaka S. Sato, Hiroyuki Kokawa, Kazutaka Okamoto, Satoshi Hirano, Masahisa Inagaki, Rapid formation of the sigma phase in 304 stainless steel during friction stir welding, *Scripta Materialia* 49 (2003) 1175–1180.
- [39] C. Hamilton, S. Dymek, A. Sommers, A thermal model of friction stir welding in aluminum alloys, *International Journal of Machine Tools & Manufacture* 48 (2008) 1120–1130.
- [40] C. Hamilton, A. Sommers, S. Dymek, A thermal model of friction stir welding applied to Sc-modified Al–Zn–Mg–Cu alloy extrusions, *International Journal of Machine Tools & Manufacture* 49 (2009) 230–238.